

# SCIENTIFIC REPORTS



OPEN

## An invertebrate-specific and immune-responsive microRNA augments oyster haemocyte phagocytosis by targeting CgI $\kappa$ B2

Received: 28 October 2015

Accepted: 22 June 2016

Published: 12 July 2016

Hao Chen<sup>1,2</sup>, Zhi Zhou<sup>1</sup>, Hao Wang<sup>1</sup>, Lingling Wang<sup>3</sup>, Weilin Wang<sup>1,2</sup>, Rui Liu<sup>1</sup>, Limei Qiu<sup>1</sup> & Linsheng Song<sup>3</sup>

Nuclear factor (NF)- $\kappa$ B pathway is an evolutionally conserved pathway in activating immune response, in which I $\kappa$ Bs can repress the activation. In the present study, cgi-miR-2d, an invertebrate-specific microRNA, was proved to regulate CgI $\kappa$ B2 expression and haemocyte phagocytosis during bacterial infection in oyster *Crassostrea gigas*. The expression of cgi-miR-2d was significantly up-regulated after *Vibrio splendidus* challenge, while CgI $\kappa$ B2 transcripts decreased. Significant decreases in both luminescence and CgI $\kappa$ B2 3'UTR level was observed after transfection of cgi-miR-2d in CgI $\kappa$ B2 3'UTR luciferase reporter assay. CgI $\kappa$ B2 mRNA level decreased significantly (0.51-fold of control group,  $p < 0.05$ ) in gain-of-function assay of cgi-miR-2d *in vivo* while it increased markedly (1.27-fold,  $p < 0.05$ ) when cgi-miR-2d was repressed (0.10-fold,  $p < 0.01$ ). A significant increase of haemocyte phagocytosis rate was observed in cgi-miR-2d overexpression group ( $p < 0.01$ ), consistent with results in CgI $\kappa$ B2 knock-down group ( $p < 0.01$ ). Moreover, the apoptosis rate of haemocytes was found significantly declined (28.57%,  $p < 0.01$ ) in gain-of-function assay of cgi-miR-2d. Together, those results not only depicted the functional conservation of miR-2d family in anti-apoptosis of oysters but also highlighted its interaction with phagocytosis by modulating NF- $\kappa$ B pathway, which might dedicate critically to the well-balance of host immune response.

Phagocytosis of immunocytes is an essential process in host immune response against invaded pathogens<sup>1</sup>. As a highly integrated cellular activity, it comprises a series of events, including pathogen recognition by cell surface receptors, intracellular signal transduction, cytoskeletal rearrangement, particle engulfment, microbial lysogenesis and antigen presentation to other immunocytes<sup>2</sup>. The phagocytosis against infiltrated pathogens, as found, can be robustly activated after challenge and strictly modulated afterward by diverse genes or pathways, keeping the well-balance of host immune system<sup>3</sup>. Among those regulators, nuclear factor- $\kappa$ B (NF- $\kappa$ B) family<sup>4</sup> is the most important ones as a global activator of phagocytosis-related genes<sup>5</sup>.

In mammals, the NF- $\kappa$ B family is mainly composed by a family of five structurally related transcriptional factors, including NF- $\kappa$ B1 (p105/p50), NF- $\kappa$ B2 (p100/p52), RelA (p65), RelB, and c-Rel<sup>5,6</sup>. Those NF- $\kappa$ B proteins dimerize with each other to form homo- and hetero-dimers and can modulate diverse biological responses, such as phagocytosis and apoptosis, by regulating target gene transcription<sup>4,7</sup>. However, NF- $\kappa$ B/Rel proteins are normally bound with inhibitor of  $\kappa$ Bs (I $\kappa$ Bs) as an inactive form<sup>8</sup>, and can only be activated by phosphorylation of I $\kappa$ Bs, which includes I $\kappa$ B $\alpha$ , I $\kappa$ B $\beta$ , I $\kappa$ B $\gamma$ , I $\kappa$ B $\epsilon$ , I $\kappa$ B $\zeta$ , and BCL3 in the mammals<sup>9</sup>. Moreover, the pre-formed NF- $\kappa$ B-DNA complex during gene transcription can also be dissociated rapidly by free nuclear I $\kappa$ Bs, attenuating the immune responses of the host<sup>9</sup>. The interaction between NF- $\kappa$ B proteins and I $\kappa$ Bs is therefore decisive in maintaining homeostasis of host and are found rigorously modulated during challenge at multiple level, including transcriptional and post-transcriptional ones<sup>4-6,9</sup>.

<sup>1</sup>Key Laboratory of Experimental Marine Biology, Institute of Oceanology, Chinese Academy of Sciences, Qingdao 266071, China. <sup>2</sup>University of Chinese Academy of Sciences, Beijing 100049, China. <sup>3</sup>Key Laboratory of Mariculture & Stock enhancement in North China's Sea, Ministry of Agriculture, Dalian Ocean University, Dalian 116023, China. Correspondence and requests for materials should be addressed to L.W. (email: wanglingling@dlo.edu.cn) or L.S. (email: lshsong@dlo.edu.cn)

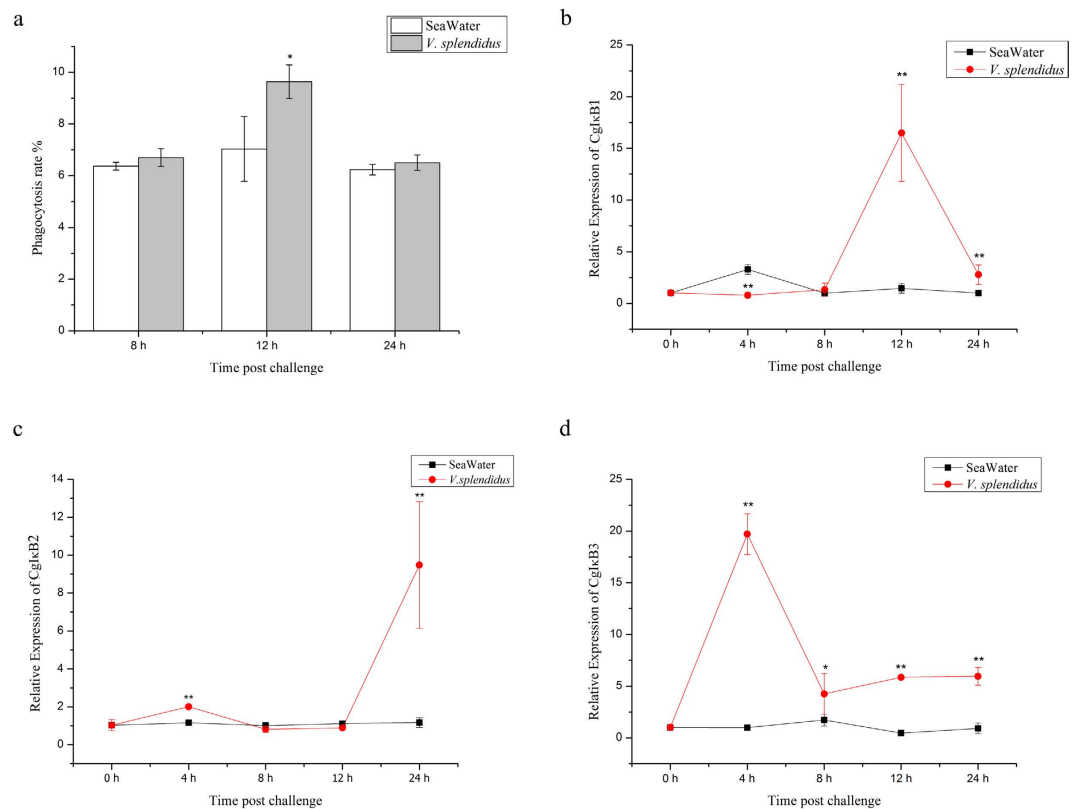


**Figure 1. Alterations of haemocyte phagocytosis rate and CgIκBs expression levels during challenge.** The phagocytosis rates of oyster haemocytes at 8 h, 12 h and 24 h after *V. splendidus* challenge were determined using flow cytometry (a). Expression levels of CgIκB1 (b), CgIκB2 (b) and CgIκB3 (c) during infection were also investigated by qRT-PCR. Significant differences were marked with asterisk “\*” if  $p < 0.05$  or “\*\*” if  $p < 0.01$ .

miRNAs are an important class of short endogenous single-stranded non-coding RNAs (~22 nt in length) which could regulate gene expression at post-transcriptional level<sup>10</sup>. Since first found in *Caenorhabditis elegans*, more than 35,828 mature miRNAs have been identified so far in over 223 species<sup>11</sup>. Though structured similarly, miRNAs diversify greatly in their function. And almost all biological processes could be modulated by miRNAs, especially those immune-related processes<sup>12,13</sup>. For example, it was found that miRNAs induced after pathogen challenge could repress the synthesis and release of cytokines while other immune-related events such as phagocytosis, migration could also be modulated by those regulators<sup>14–16</sup>. Recently, miRNA-mediated modulation were likewise observed in multiple immune-related pathways, including NF-κB pathway<sup>17</sup>. For instance, miR-199a, a miRNA down-regulated in endometriosis, was proved to inhibit the IκB kinase β in embryonic stem cells and suppress the NF-κB pathway activation and interleukin-8 expression afterward<sup>18</sup>. Some other miRNAs such as miR-146a, miR-155, miR-181b and miR-21 were also annotated as regulators of NF-κB pathway<sup>17</sup>. Although mass of reports have revealed the interaction between miRNAs and NF-κB pathway in mammals, less is investigated in invertebrates<sup>17</sup>.

As an important intertidal bivalve, oyster *Crassostrea gigas* suffers continuously from harsh environments and surrounding pathogens<sup>19</sup>. A robust immune response to fast eliminate invaded bacteria is therefore greatly needed<sup>20–22</sup>. With the release of genome information, oysters have been gradually regarded as a model in investigating invertebrate immune system with some components of NF-κB pathway characterized in the past decades, including one Rel and three IκBs<sup>23–26</sup>. Meanwhile, more than fifty immune-responsive miRNAs have been identified in *C. gigas*, among which cgi-miR-2d (Supplementary Fig. S1) was predicted as a modulator of CgIκB2<sup>27</sup>. The purposes of the present study were therefore to (1) survey the phagocytic changes of oyster haemocytes after *Vibrio splendidus* challenge, (2) revise the phylogeny of cgi-miR-2d, (3) investigate the interaction between CgIκBs and cgi-miR-2d during challenge, and (4) reveal the modulation on haemocyte phagocytosis by cgi-miR-2d and hopefully provide new hints for the miRNA-mediated immunomodulation mechanism in oysters.

## Results

### Changes in haemocyte phagocytosis and CgIκBs expression during *V. splendidus* stimulation.

The phagocytosis rate of oyster haemocytes was determined at 8 h, 12 h and 24 h post *V. splendidus* challenge. As a result, it remained unchanged at 8 h and 24 h post stimulation and increased significantly at 12 h (9.63% in challenge group *verse* 7.03% in seawater control group,  $p < 0.01$ ) (Fig. 1a).

The expression level of CgIκB1 in oyster haemocytes decreased at 4 h post challenge yet recuperated afterward at 8 h. A transcriptional summit of CgIκB1 was then observed at 12 h post challenge ( $p < 0.01$ ) (Fig. 1b). On the

Previous ID	Present ID	Sequence (5'-3')
cgi-miR-2e	cgi-miR-2a-1	UAUCACAGCCAGCUUUGAUGA
cgi-miR-2d	cgi-miR-2a-2	UAUCACAGCCAGCUUUGAUGACA
cgi-miR-2b	cgi-miR-2b-1	UAUCACAGCUAGCUUUGAUGAGCU
cgi-miR-2c	cgi-miR-2b-2	GAUCACAGCCAGCUUUGAUGAG
cgi-miR-2a	cgi-miR-2d	UAUCACAGCCUGCUUGGAUCAGU

**Table 1. Homologues of miR-2 family in oyster.**

contrary, the CgIkB2 transcripts were found up-regulated robustly at 4 h post *V. splendidus* injection (2.00-fold of that in the control group,  $p < 0.01$ ) and decreased at 8 h (Fig. 1c). No significant changes in CgIkB2 mRNA level were observed at 12 h until it ascended markedly at 24 h post injection, which reached 9.48-fold of that in control group at 0 h ( $p < 0.01$ ) (Fig. 1c). The expression level of CgIkB3 also peaked at 4 h post challenge, and kept at a relatively higher level from 8 h to 24 h ( $p < 0.01$ ) (Fig. 1d).

**Expression alternation of cgi-miR-2d during *V. splendidus* challenge.** Five members of miR-2 family in oyster were first subjected to miRBase (<http://www.mirbase.org>) in search of homologues and were renamed subsequently according to their sequence similarity (Table 1). Consequently, a remarkable nucleotide similarity was observed among oyster miR-2 family members (Fig. 2a). Meanwhile, there was a great diversity within homologues of miR-2d from different organisms (Table 2) where cgi-miR-2d was highly conserved with that from *Lottia gigantean* (Fig. 2b). Moreover, all miR-2d were found derived from the 3' arm of their precursor.

The expression changes of cgi-miR-2d during *V. splendidus* challenge were investigated subsequently. As a result, cgi-miR-2d transcripts were found increased rapidly after the challenge and peaked at 8 h post injection (3.32-fold of that in the control group,  $p < 0.01$ ) (Fig. 2c). Though descended afterward, they still maintained at 1.41-fold of that in seawater control group ( $p < 0.01$ ). No significant changes of the cgi-miR-2d transcripts were observed in seawater control group during the experiment (Fig. 2c).

**The interaction between cgi-miR-2d and CgIkB2 *in vitro*.** CgIkB2 3'UTR (291 bp in length) containing putative binding site of cgi-miR-2d (from 84 to 105 nt, Fig. 2d) was first cloned using gene-specific primer and inserted subsequently into the psiCHECK-2 vector (designated as wild type vector) for luciferase reporter assays in HEK293T cells. At 24 h post transfection, the relative luminescence ratio in each group was detected and a significant decrease was observed in cgi-miR-2d group (32.40%) in comparison with that in blank or miRNA control group ( $p < 0.05$ ) (Fig. 2e). Similarly, the decrease in relative luminescence ratio could also be observed in positive control group (binding site from 40 to 59 nt,  $p < 0.05$ ) (Fig. 2d,e). To further verify the binding specificity of cgi-miR-2d, mutation was made on the CgIkB2 3'UTR (designated as mutated type) where was complementary with seed region of cgi-miR-2d (Fig. 2d). Consequently, no significant changes were observed in relative luminescence ratio of cgi-miR-2d group while it decreased significantly in positive control group ( $p < 0.05$ ) (Fig. 2f).

The relative expression level of CgIkB2 3'UTR was subsequently measured in cells transfected with wild type vector by quantitative real-time PCR (qRT-PCR). Consistently, CgIkB2 3'UTR decreased significantly in both cgi-miR-2d group (0.84-fold of that in miRNA control group,  $p < 0.05$ ) and positive control group (0.35-fold of that in miRNA control group,  $p < 0.05$ ) when compared to that in blank or miRNA control group (Fig. 2g).

**The interaction between cgi-miR-2d and CgIkB2 *in vivo* and modulation on phagocytosis rate and apoptosis rate.** Gain- and loss-of-function assay of cgi-miR-2d were subsequently conducted *in vivo* by injecting cgi-miR-2d mimics and inhibitors into oysters. The cgi-miR-2d transcripts were first investigated at 24 h post injection. Consequently, a significant increase of cgi-miR-2d transcripts was observed in cgi-miR-2d group (2.49-fold of that in seawater group,  $p < 0.05$ ) (Fig. 3a) while they decreased robustly when cgi-miR-2d inhibitors were injected (0.10-fold of seawater control group,  $p < 0.05$ ) (Fig. 3a). However, no significant changes of CgIkB1 or CgIkB3 transcripts were observed in either group at 24 h post injection (Fig. 3b,d). Comparatively, CgIkB2 transcripts decreased simultaneously in cgi-miR-2d group (0.51-fold of seawater group,  $p < 0.05$ ) while increased significantly to 1.27-fold in cgi-miR-2d inhibitor group when compared with seawater group ( $p < 0.05$ ) (Fig. 3c).

Alternations in phagocytosis and apoptosis rate of oyster haemocytes were also surveyed. It turned out that haemocyte phagocytosis rate increased after cgi-miR-2d overexpression (2.83%,  $p < 0.05$ ) and decreased when cgi-miR-2d was repressed by its inhibitor (1.16%,  $p < 0.05$ ), in comparison with that in seawater group (2.10%, Fig. 3e). In addition, a significant decrease of phagocytosis rate was observed at 24 h after *V. splendidus* challenge (Fig. 3e). The apoptosis rate of haemocytes was down-regulated significantly (28.57%,  $p < 0.05$ ) after gain-of-function assay of cgi-miR-2d whereas it remained unchanged after cgi-miR-2d inhibition (Fig. 3e). The apoptosis rate of haemocytes in bacteria challenge group, however, decreased remarkably at 24 h ( $p < 0.05$ ) (Fig. 3e).

**Haemocyte phagocytic and apoptotic changes after CgIkB2 knock-down assay *in vivo*.** DsRNA of CgIkB2 was synthesized *in vitro* using a fragment from CgIkB2 coding region which was unique in genome and injected into oysters for knock-down assay *in vivo* (Fig. 4a, Supplementary Fig. S2). The expression level of CgIkB2 in siCgIkB2 group was surveyed at 24 h post injection and was found declined remarkably (0.48-fold of that in siEGFP group,  $p < 0.05$ ) (Fig. 4b). Correspondingly, the phagocytosis rate increased significantly in siCgIkB2 group when compared with that in siEGFP group (3.00% *verse* 0.90%,  $p < 0.05$ ) (Fig. 4c). And the

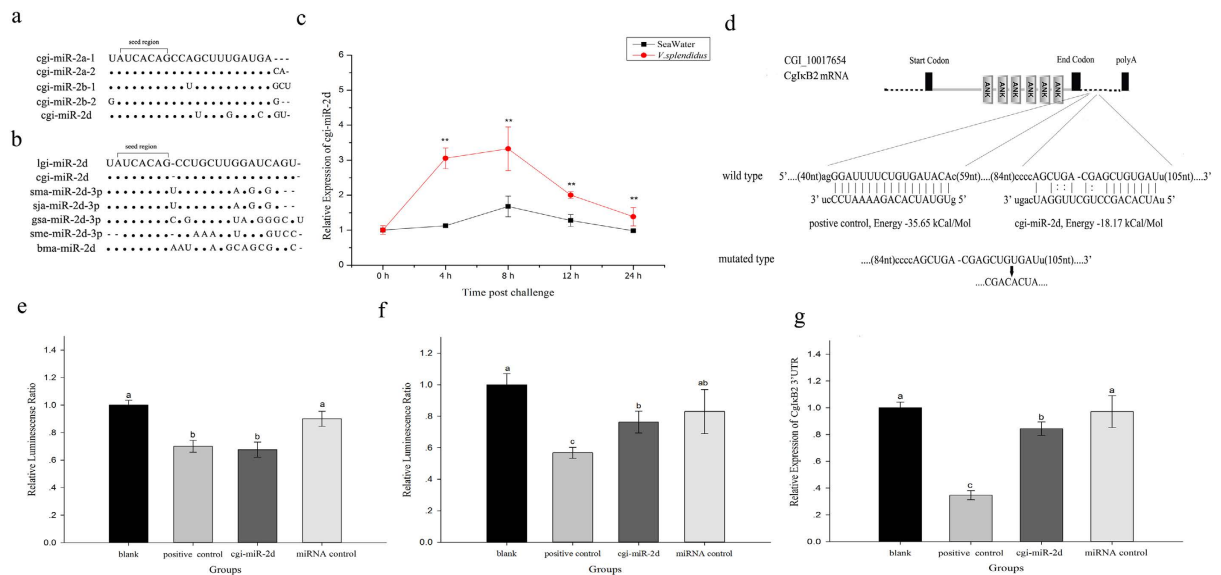


**Figure 2. Interaction between cgi-miR-2d and CgIkB2 *in vitro*.** The sequence similarity of members in oyster miR-2 family (including cgi-miR-2d) was illustrated by Cluster X (a). Nucleotide diversity could be found in miR-2d from *Lottia gigantean* (lgi), *Schistosoma mansoni* (sma), *Schistosoma japonicum* (sja), *Gyrodactylus salaris* (gsa), *Schmidtea mediterranea* (sme) and *Brugia malayi* (bma) while cgi-miR-2d was highly conserved with that in *L. gigantean* (b). The expression alternations of cgi-miR-2d were surveyed during *V. splendidus* challenge by qRT-PCR (c). Target genes of cgi-miR-2d were searched globally by miRanda and a binding site was found at CgIkB2 3'UTR (d). Luciferase reporter assay was subsequently conducted using wild type 3'UTR (e) or mutated type 3'UTR (f). The relative expression level of CgIkB2 3'UTR in cells transfected with wild type 3'UTR were also surveyed at 24 h post transfection (g). Significant differences were marked with letters (a, b, c etc.) if  $p < 0.05$  or “\*\*” if  $p < 0.01$ .

Specie	ID	Sequence (5'-3')
<i>Gyrodactylus salaris</i>	gsa-miR-2d-3p	UAUCACAGCCGUGCUUUAAGGGCUU
<i>Brugia malayi</i>	bma-miR-2d	UAUCACAGAAUUGAUGCAGCGAGC
<i>Schistosoma mansoni</i>	sma-miR-2d-3p	UAUCACAGUCCUGCUUAGGUGA
<i>Schistosoma japonicum</i>	sja-miR-2d-3p	UAUCACAGUCCUGCUUAGGUGA
<i>Lottia gigantean</i>	lgi-miR-2d	UAUCACAGCCUGCUUGGAUCAGU
<i>Schmidtea mediterranea</i>	sme-miR-2d-3p	UCACAGCCAAAUUUGAUGUCC
<i>Crassostrea gigas</i>	cgi-miR-2d	UAUCACAGCCUGCUUGGAUCAGU

**Table 2. Sequences of miR-2d from different species.**

haemocyte apoptosis rate decreased after the interference of CgIkB2 in comparison with that in siEGFP control group ( $p < 0.05$ ) (Fig. 4c).

## Discussion

Phagocytosis against bacteria has been regarded as a fundamental event in host immune process and contributes greatly to the homeostasis of organism during pathogen challenge<sup>21</sup>. It has been observed that phagocytosis of molluscan haemocytes could also be rapidly triggered after stimulation and dedicate to the fast elimination of invaded microbes<sup>22,28,29</sup>. In the present study, the phagocytosis rate of oyster haemocytes also increased significantly at 12 h post *V. splendidus* challenge (Fig. 1a) and declined afterward. The spontaneous alternation in haemocyte phagocytosis highlighted the intense immune response inside the oysters and indicated the rigorous modulation beneath.

Within mass of immune-related pathways, the NF- $\kappa$ B pathway has been well investigated as a global regulator of immune response including phagocytosis, where  $\kappa$ B genes are regarded as hallmarks<sup>4</sup>. Here, the expression levels of three CgIkBs in haemocytes were also surveyed during challenge in reflection of NF- $\kappa$ B activation. As a result, three CgIkBs were rigorously modulated during challenge (Fig. 1b–d) with different expression pattern, which was similar with previous findings<sup>25,26</sup>, demonstrating the dynamic involvement of NF- $\kappa$ B pathway in immune response of mollusk as well as the functional distinctions among CgIkBs<sup>30</sup>. Moreover, an opposite alternation pattern was observed between the CgIkB2 transcripts and haemocyte phagocytosis (Fig. 1a,c). Given the interaction between phagocytosis and NF- $\kappa$ B pathway in mammals, we deduced audaciously that oyster phagocytosis could also be modulated by CgIkB2. Correspondingly, the phagocytosis rate of oyster haemocytes increased

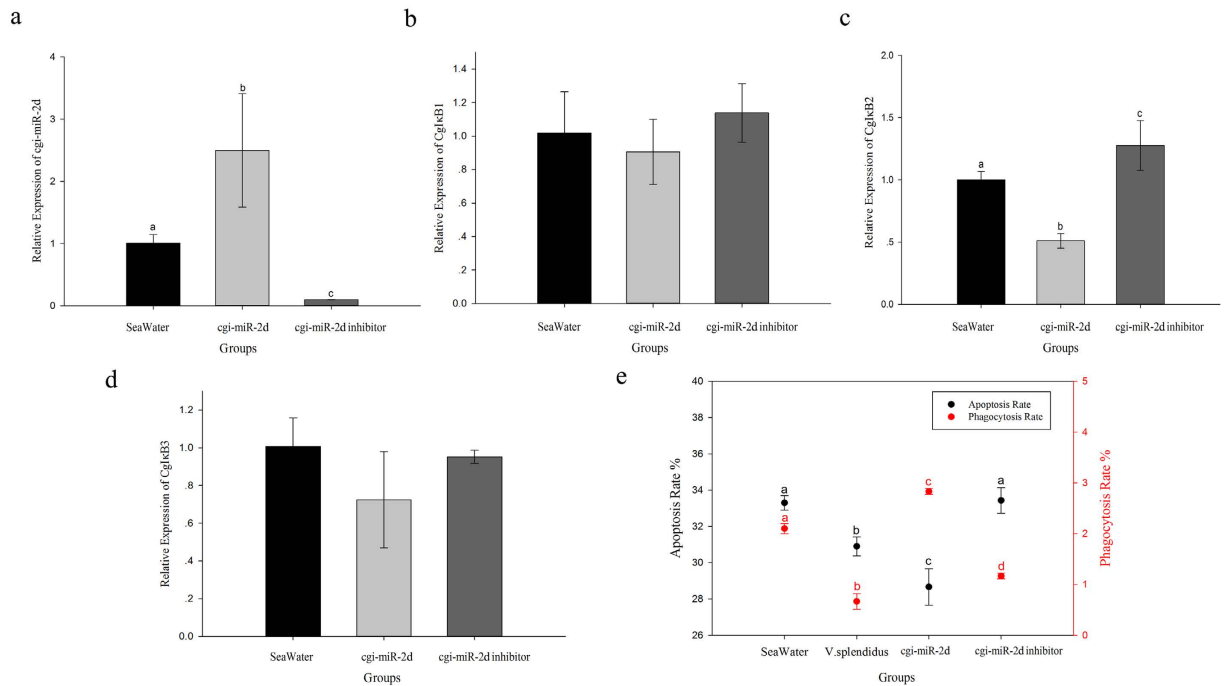


**Figure 3. Alterations of CgIκBs mRNA and haemocyte phagocytosis and apoptosis rate in gain- and loss-of-function assay of cgi-miR-2d *in vivo*.** Gain- and loss-of-function assay were conducted *in vivo* by injection of cgi-miR-2d mimics or inhibitors. cgi-miR-2d transcripts were firstly surveyed at 24 h post injection by qRT-PCR (a). Expression alternations of CgIκB1 (b), CgIκB2 (c) and CgIκB3 (d) were also investigated. Haemocyte phagocytosis and apoptosis rate were investigated using flow cytometry simultaneously (e). Significant differences were marked with different letters (a, b, c etc.) if  $p < 0.05$ .

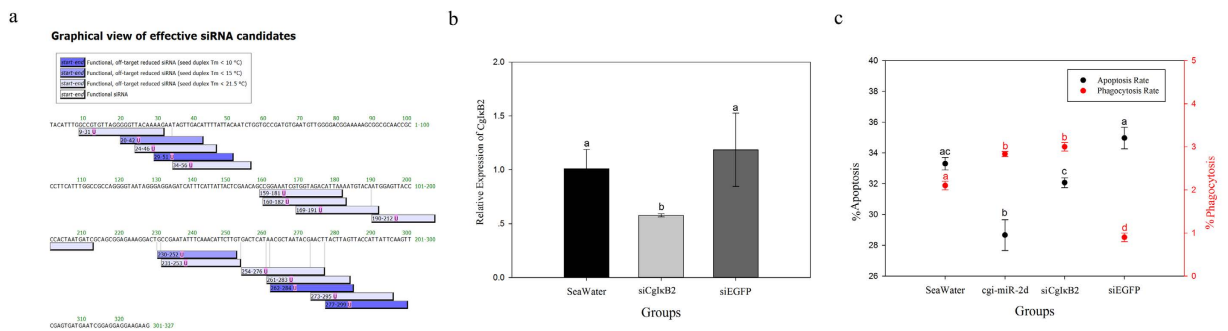


**Figure 4. Alterations of CgIκB2 mRNA and haemocyte phagocytosis and apoptosis rate after knock-down of CgIκB2 *in vivo*.** Knock-down of CgIκB2 was conducted *in vivo* by injection of dsRNA designed by <http://sidirect2.rnai.jp/> with default settings (a). Expression changes of CgIκB2 mRNA were detected by qRT-PCR at 24 h post the injection (b). Phagocytosis and apoptosis rate of haemocytes were also surveyed (c). Significant differences were marked with different letters (a, b, c etc.) if  $p < 0.05$ .

significantly in CgIκB2 knock-down assay *in vivo* (Fig. 4a,b), confirming our speculations above. Paradoxically, CgIκB2 remained at basal level at 12 h post challenge, suggesting the existence of post-transcription regulation. Within the expectation, cgi-miR-2d, a putative regulator of CgIκB2, was found up-regulated markedly during bacteria challenge (Fig. 2c). The interaction between cgi-miR-2d and CgIκB2 was then verified both *in vitro* and *in vivo*.

To date, mass of miRNAs has been identified and proved crucial in diverse biological processes, especially in immune response<sup>31</sup>. It was also suggested that majority of miRNAs could regulate target genes post-transcriptionally by binding to their 3'UTR region<sup>17,32</sup>. The putative modulation by cgi-miR-2d was first confirmed *in vitro* by CgIκB2 3'UTR luciferase reporter assay in HEK293T cells (Fig. 2d). Consequently, an intense depression of relative luminescence ratio was observed when cgi-miR-2d was co-transfected with wild type CgIκB2 3'UTR (Fig. 2e) while it remained unchanged when the binding site of cgi-miR-2d at 3'UTR was mutated (Fig. 2f). Besides, some reports have also found that the transcripts of target genes could be degraded partly

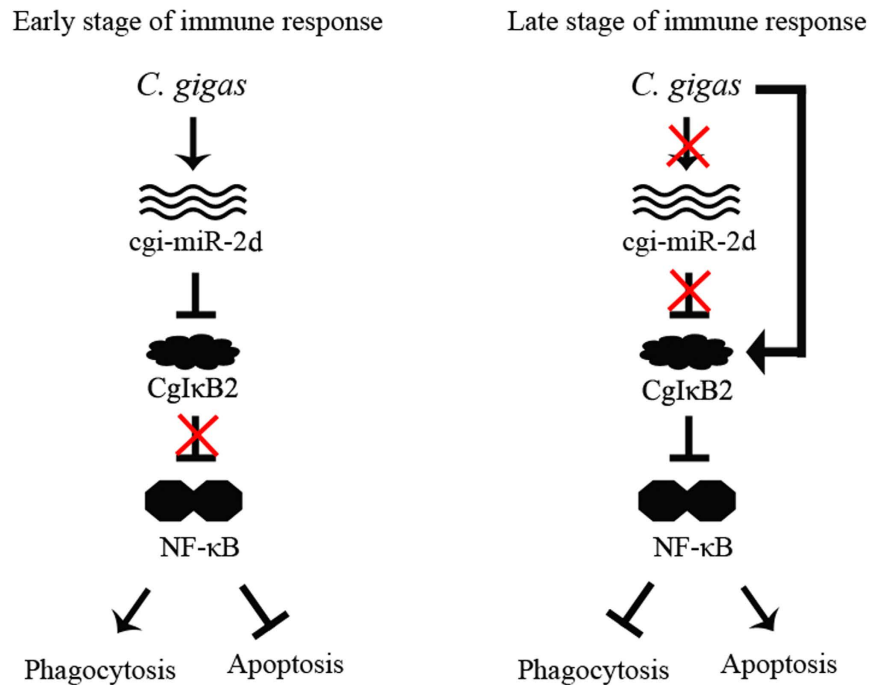


**Figure 5. Proposed role of cgi-miR-2d in oyster immune response by targeting CgI $\kappa$ B2.** Given the expression changes of cgi-miR-2d and CgI $\kappa$ B2, it was suggested that CgI $\kappa$ B2 could be modulated post-transcriptionally by up-regulated cgi-miR-2d at the early stage of *V. splendidus* infection and led to the inhibition of NF- $\kappa$ B pathway activation as well as the promotion of haemocyte phagocytosis. At the late stage of *V. splendidus* challenge, expression of cgi-miR-2d was repressed while that of CgI $\kappa$ B2 was up-regulated to disadvantage both NF- $\kappa$ B pathway and haemocyte phagocytosis. Moreover, apoptosis could also be regulated by cgi-miR-2d, which was conserved among miR-2 family yet not dominant during *V. splendidus* challenge, indicating the existence of other unknown modulatory pathways.

by miRNA in imprecise complementation with their 3'UTR<sup>33</sup>, or completely when miRNAs were in complete complementation<sup>34,35</sup>. Herein, similar results could also be observed where CgI $\kappa$ B2 3'UTR transcripts decreased in both positive control and cgi-miR-2d group (Fig. 2g), reconfirming the interaction between CgI $\kappa$ B2 3'UTR and cgi-miR-2d *in vitro*. The interaction between cgi-miR-2d and CgI $\kappa$ B2 was then verified *in vivo* by gain- and loss-of-function assay of cgi-miR-2d. Consistently, the expression level of CgI $\kappa$ B2 decreased significantly during gain-of-function assay of cgi-miR-2d *in vivo*, and increased when endogenous cgi-miR-2d was repressed by its inhibitor (Fig. 3a,c). Meanwhile, no significant changes of CgI $\kappa$ B1 or CgI $\kappa$ B3 transcripts were observed in gain- and loss-of-function assay of cgi-miR-2d (Fig. 3b,d). Collectively, those results confirmed the interaction between cgi-miR-2d and CgI $\kappa$ B2, which might dedicate crucially in modulating host immune response.

As mentioned, massive reports in mammals have revealed the interaction between NF- $\kappa$ B pathway and phagocytosis<sup>36–38</sup>. Recently, report in *Apostichopus japonicus* has also depicted the participation of miRNAs in haemocytes phagocytosis<sup>12</sup>. Given that CgI $\kappa$ Bs could repress NF- $\kappa$ B activation *in vitro*<sup>25,26</sup>, the interaction between cgi-miR-2d and CgI $\kappa$ B2 was therefore supposed to augment haemocyte phagocytosis by modulating NF- $\kappa$ B pathway. Unexpectedly, a significant increase of phagocytic rate was observed in cgi-miR-2d overexpression group (Fig. 3c), which was similar with that in CgI $\kappa$ B2 knock-down group (Fig. 4c). And the increase caused by cgi-miR-2d could also be reversed by cgi-miR-2d inhibitors (Fig. 3c), accompanying with increase of CgI $\kappa$ B2 transcripts. Among the numerous miRNAs identified from diverse species<sup>39</sup>, miR-2 family was found expressed exclusively in invertebrates and could promote cell survival<sup>40</sup>. In the meantime NF- $\kappa$ B pathway has also been well-known in anti-apoptosis in either oysters (Fig. 4c) or mammals<sup>7,37,38</sup>. Thence, alternations on haemocyte apoptosis rate were surveyed simultaneously. Accordingly, it decreased significantly after gain-of-function assay of cgi-miR-2d *in vivo* and increased when cgi-miR-2d was inhibited (Fig. 4c). However, the apoptosis rate decreased remarkably after *V. splendidus* challenge, suggesting a more complicated modulation network during stimulation. Nevertheless, these results verified the interaction between cgi-miR-2d and CgI $\kappa$ B2 and depicted their contribution on the phagocytosis rate of haemocytes. Given to the expression changes of cgi-miR-2d and CgI $\kappa$ B2, their interaction might also dedicate importantly to oysters immune response during bacteria challenge (Fig. 5)<sup>27</sup> as well as the oysters' thriving in intertidal regions.

## Materials and Methods

**Oyster culture, bacteria challenge and sample collection.** Oysters *C. gigas* (averaging 150 mm in shell length, 70 mm in width) engaged in this experiment were collected from a local farm in Qingdao, China. A narrow notch was sawed in the oyster shell where was close to the adductor muscle for subsequent injection<sup>20</sup>. All oysters were then acclimatized in aerated sea water (about 20 °C) for two weeks before use.

Category	Primer and RNA name	Sequence (5'-3')
RNAs	cgi-miR-2d mimics	UAUCACAGCCUGCUUGGAUCAGU UGAUCCAAGCAGGCUGUGAUUU
	Positive control	GUGUAUCACAGAAAUCCCU GGAUUUUCUGUGAUACACUU
	miRNA control	UUCUCCGAACGUGUCACGUTT ACGUGACACGUUCGGAGAATT
	cgi-miR-2d inhibitor	ACUGAUCCAAGCAGGCUGUGAUUA
UTR clone primers	CgIκB2_UTRclone_F	TATTACAATCTGGTGCCGATGTGA
	AP-dT	GGCCACGCTCGACTAGTACT <sub>17</sub>
	CgIκB2_mutate_F	AGCTGACGACGACACTATGGCTGATG
	CgIκB2_mutate_R	ACAATCAGCCATAGTGTCTGTCGTCAGC
Recombination primers	CgIκB2_XhoI	CTCGAGAGAAAGGACTGCCGAA
	CgIκB2_NotI	GCGGCCGCTTTAGACTTGTC
RNAi clone primers	siCgIκB2_basic_F	AGACCCATGCAAAATCTGGAC
	siCgIκB2_basic_R	CTTCTTCTCCTCCGATTTCATC
	siCgIκB2_T7_F	TAATACGACTCACTATAGGGATC AGACCCATGCAAAATCTGGAC
	siCgIκB2_T7_R	TAATACGACTCACTATAGGGATC CTTCTTCTCCTCCGATTTCATC
	siEGFP_basic_F	CGACGTAAACGGCCACAAGT
	siEGFP_basic_R	CTTGTACAGCTCGTCCATGC
	siEGFP_T7_F	TAATACGACTCACTATAGGGA TCCGACGTAAACGGCCACAAGT
	siEGFP_T7_R	TAATACGACTCACTATAGGGATC CTTGTACAGCTCGTCCATGC
Real-Time primers	GAPDH_F	AGGTCGGTGTGAACGGATTTG
	GAPDH_R	TGTAGACCATGTAGTTGAGGTCA
	EF-F	AGTACCAAGGCTGCACAGAAAG
	EF_R	TCCGACGTATTCTTTGCGATGT
	CgIκB1_RT_F	CCCTTCACATTGCCAGTAG
	CgIκB1_RT_R	ATTGGGAGATGGGTGTTCT
	CgIκB2_RT_F	CGAGTGATGAATCGGAGGAGG
	CgIκB2_RT_R	CACACAATCAGCCAATCACAGC
	CgIκB3_RT_F	ACCTCCCCTCCCTACAACCTCAGACT
	CgIκB3_RT_R	CCTGGTGACATGGAATGGGCAACT
	cgi-miR-2d	TATCACAGCCTGCTTGGATCAGT
	rRNA_5s	CAAGGATGACACGCAAAT

**Table 3. Primers and RNAs used in this study.**

A total of 30 oysters were employed for bacteria stimulation to investigate expression changes of cgi-miR-2d identified previously<sup>27</sup>. Briefly, oysters in PBS control group and *V. splendidus* challenge group were injected with 100 µL of phosphate buffered saline (PBS, 0.14 mol L<sup>-1</sup> sodium chloride, 3 mmol L<sup>-1</sup> potassium chloride, 8 mmol L<sup>-1</sup> disodium hydrogen phosphate dodecahydrate, 1.5 mmol L<sup>-1</sup> potassium phosphate monobasic, pH 7.4) and 100 µL suspension of alive *V. splendidus* strain<sup>41</sup> (1 × 10<sup>7</sup> CFU mL<sup>-1</sup> in PBS), respectively. At 12 h later, haemocytes from five oysters in each group were collected from cardiocoelom by centrifugation at 800 g, 4 °C for 10 minutes and pooled together for subsequent miRNA extraction and qRT-PCR analysis of cgi-miR-2d. Another 360 oysters were also employed for bacteria challenge. Similarly, oysters in seawater control group and *V. splendidus* challenge group were stimulated with 100 µL sterile seawater and 100 µL suspension of live *V. splendidus* strain (1 × 10<sup>7</sup> CFU mL<sup>-1</sup> in sterile seawater), respectively. Haemocytes from five oysters in each group were collected at 0, 4, 8, 12 and 24 h post injection, and pooled together for subsequent RNA extraction and qRT-PCR analysis of CgIκBs. Haemocytes from another five individuals were also sampled for quantitative analysis of cgi-miR-2d. Additional five oysters in each group were sampled likewise at 8, 12 and 24 h post injection for the analysis of haemocyte phagocytic rate.

All trials were conducted with three biological replicates.

**RNA isolation, cDNA synthesis and SYBR Green fluorescent qRT-PCR.** RNA isolation and cDNA synthesis were conducted using methods in previous reports<sup>42</sup>. The SYBR Green fluorescent qRT-PCR was carried out in an ABI 7500 Real-time Thermal Cycler according to the manual (Applied Biosystems). The gene-specific primers were designed according to its cDNA sequences and listed on Table 3. Briefly, a reaction mix with 5 µL of 2 × SYBR Green Master Mix (Takara), 2 µL of the diluted cDNA templates, 0.2 µL of each primers (10 mmol L<sup>-1</sup>), 0.2 µL ROX Reference Dye II and 2.4 µL of DEPC water was used to amplify corresponding genes. The elongation factor (EF) gene<sup>43</sup> was used as an internal control for the expression analysis of oyster CgIκBs.

Total miRNAs were extracted using PureLink miRNA Isolation Kit (Invitrogen) according to the manufacturer's protocol. The synthesis of cDNA was conducted using miScript II RT (Qiagen) with miRNA extracted above at 37 °C for 1 h and terminated by heating at 95 °C for 5 min. The cDNA mix obtained was diluted with the addition of 200 µL RNase-free water before use. The SYBR green fluorescent qRT-PCR was carried out in a total volume of 25.0 µL, containing 12.5 µL of 2 × miScript SYBR Green PCR Master Mix (Qiagen), 2.5 µL of diluted

cDNA, 2.5  $\mu\text{L}$  of each primers (10 mmol  $\text{L}^{-1}$ ), and 5.0  $\mu\text{L}$  of RNase-free water. All primers were listed in Table 3, and the 5S rRNA was used as internal control.

All data were given in terms of relative mRNA or miRNA expression using the  $2^{-\Delta\Delta\text{Ct}}$  method<sup>44</sup>.

**Target prediction of cgi-miR-2d and 3'UTR luciferase reporter assay.** The cgi-miR-2d mimics which would alter into single strand *in vivo* and be identical with endogenous cgi-miR-2d were synthesized by GenePharma. A positive miRNA mimics with binding capability to CgIkB2 3'UTR (from 40 to 59 nt) was also synthesized. miRNA control originated from *C. elegans* and could not target any oyster genes or mimic any oyster miRNAs was as well employed. Cgi-miR-2d inhibitors which were in complete complementation with cgi-miR-2d and could sequester it by binding were synthesized for loss-of-function assay. All RNA was diluted at a final concentration of 20  $\mu\text{mol L}^{-1}$  using DEPC water before use. These RNA sequences were listed on Table 3.

Target prediction of cgi-miR-2d was conducted by miRanda using 3'UTR sequences deduced from oyster genome information<sup>19</sup>. The wild type or mutated type of CgIkB2 3'UTR was cloned with gene-specific primers (Table 3) and inserted into psiCHECK-2 vector (Promega) for subsequent luciferase reporter assay with methods described previously<sup>15</sup>. Briefly, a total of  $1 \times 10^5$  HEK293T cells were seeded into each well of 48-well plates and cultured overnight before transfection. Cells in positive control, cgi-miR-2d and miRNA control were then transfected with a mixture of 100 ng luciferase reporter plasmid (extracted by Tiangen EndoFree Maxi Plasmid Kit) and 5 pmol positive control or cgi-miR-2d mimics or miRNA control using Lipofectamine 2000 reagent (Invitrogen) according to the protocol. Cells transfected merely with recombinant vector were employed as blank group. The detailed information was listed on Supplementary Table S1.

The luciferase activities in those groups were measured at 24 h post transfection according to the manufacturer's instruction using Dual-Luciferase Reporter Assay System kit (Promega). Briefly, cells in each well were firstly lysed using Passive Lysis Buffer provided by the kit. A total of 100  $\mu\text{L}$  LARII was then added into 20  $\mu\text{L}$  cell lysates to detect the firefly luciferase activity using luminometer. And a volume of 100  $\mu\text{L}$  Stop & Glo Reagent was added into the mixture to measure renilla luciferase activity. Cells transfected with wild type 3'UTR were also harvested for quantitative real-time PCR of CgIkB2 3'UTR with GAPDH as the internal control. Each trial was conducted with three replicates.

**Gain- and loss-of-function assay of cgi-miR-2d *in vivo*.** A number of 90 oysters were employed for gain- and loss-of-function assay and randomly divided into three groups (designated as seawater, cgi-miR-2d and cg-miR-2a inhibitor group), receiving an injection of 100  $\mu\text{L}$  sterile seawater, 2.5 nmol cgi-miR-2d mimics (in 100  $\mu\text{L}$  sterile seawater) and 2.5 nmol cgi-miR-2d inhibitors (in 100  $\mu\text{L}$  sterile seawater), respectively. Haemocytes from five oysters in each group were collected afterward at 24 h post injection to survey expression changes of CgIkBs. The phagocytosis and apoptosis rate of haemocytes were also surveyed at the same time using another five oysters. Oysters challenged with *V. splendidus* for 24 h (designated as *V. splendidus* group) were also employed and subjected for phagocytosis and apoptosis assay. Each trial was conducted with three replicates.

**CgIkB2 knock-down assay *in vivo*.** DsRNA synthesis was conducted using method described in previous reports<sup>45</sup>. Briefly, a fragment from CgIkB2 coding region (85 nt to 474 nt) which was unique among oyster coding genes was firstly cloned and subjected to siDirect2 (<http://sirect2.rnai.jp/>) for siRNA prediction. A pair of T7 promoter linked primer was then employed for *in vitro* transcription of CgIkB2 dsRNA. A DNA fragment (657 bp) from pEGFP-N1 vector (Clontech) was also cloned to synthesize control dsRNA<sup>45</sup>.

A total of 90 oysters were employed and randomly divided into three groups for subsequent knock-down experiment. Oysters in seawater group, siCgIkB2 group and siEGFP group were injected with 100  $\mu\text{L}$  sterile seawater, 100  $\mu\text{g}$  dsRNA of IkB (in 100  $\mu\text{L}$  sterile seawater) and 100  $\mu\text{g}$  dsRNA of EGFP (in 100  $\mu\text{L}$  sterile seawater), respectively, and the haemocytes were sampled from cardiocoelom at 24 h later to detect expression changes of CgIkB2. The haemocytes from another five oysters in each group were also collected for phagocytic and apoptosis detection. All the trials were conducted with three parallel replicates.

**Determination of haemocyte phagocytosis and apoptosis rate.** Phagocytosis rate was determined using the method modified from previous report<sup>20</sup>. In brief, *V. splendidus* cultured at 16 °C overnight was labeled by FITC (Sigma) and diluted to  $10^8$  cells  $\text{mL}^{-1}$  for later use. Oyster haemocytes collected freshly with acid citrate-dextrose anticoagulant agent (22 g  $\text{L}^{-1}$  Sodium Citrate, 8 g  $\text{L}^{-1}$  citric acid, 24.5 g  $\text{L}^{-1}$  glucose, pH 7.4) were resuspended in L15 medium (Gibco) to a final concentration of  $2 \times 10^6$  cells  $\text{mL}^{-1}$  before the incubation with the same volume of FITC-labeled *V. splendidus* for 60 min. The incubated haemocytes were then washed for three times with L15 medium to remove extracellular bacteria. After a recollection by centrifugation at 800 g, 4 °C for 5 min, haemocytes were subjected to flow cytometry (BD Biosciences) to investigate phagocytosis rate.

Haemocyte apoptosis rate was measured using the Annexin V-FITC Detection Kit (Beyotime). In brief, 200  $\mu\text{L}$  of diluted haemocytes were incubated firstly with 5  $\mu\text{L}$  of Annexin V-FITC in the dark at room temperature for 10 min and then with 10  $\mu\text{L}$  propidium iodide for 5 min. Haemocytes were also subjected to flow cytometry for apoptosis rate detection after the wash and recollection.

**Statistical analysis.** All data were given as means  $\pm$  S.D. One-way analysis of variance (one-way ANOVA) followed by a multiple comparison (LSD method) was used subsequently to determine difference. Asterisks (<sup>\*</sup> if  $p < 0.05$ , <sup>\*\*</sup> if  $p < 0.01$ ) or different letters (a, b, c etc. if  $p < 0.05$ ) were marked on the top of bar to indicate significant difference.

## References

- Underhill, D. M. & Ozinsky, A. Phagocytosis of microbes: complexity in action. *Annu Rev Immunol* **20**, 825–852 (2002).
- Steven Greenberg & Grinstein, S. Phagocytosis and innate immunity. *Curr Opin Immunol*. **14**, 136–145 (2002).
- Jutras, I. & Desjardins, M. Phagocytosis: at the crossroads of innate and adaptive immunity. *Annu. Rev. Cell Dev. Biol.* **21**, 511–530 (2005).



4. Tripathi, P. & Aggarwal, A. NF- $\kappa$ B transcription factor: a key player in the generation of immune response. *Curr Sci* **90**, 519–531 (2006).
5. Ghosh, S., May, M. J. & Kopp, E. B. NF- $\kappa$ B and Rel proteins: evolutionarily conserved mediators of immune responses. *Annu Rev Immunol* **16**, 225–260 (1998).
6. Siebenlist, U., Franzoso, G. & Brown, K. Structure, regulation and function of NF- $\kappa$ B. *Annu Rev Cell Biol* **10**, 405–455 (1994).
7. Antwerp, D. J. V., J. Martin, S., M. Verma, I. & R. Green, D. Inhibition of TNF-induced apoptosis by NF- $\kappa$ B. *Trends In Cell Biol* **8**, 107–111 (1998).
8. Baeuerle, P. & Baltimore, D. I kappa B: a specific inhibitor of the NF-kappa B transcription factor. *Science* **242**, 540–546 (1988).
9. Beg, A. A. & Baldwin, A. S. The I kappa B proteins: multifunctional regulators of Rel/NF-kappaB transcription factors. *Genes & Dev* **7**, 2064–2070 (1993).
10. Bartel, D. P. MicroRNAs: genomics, biogenesis, mechanism, and function. *Cell* **116**, 281–297 (2004).
11. Kozomara, A. & Griffiths-Jones, S. miRBase: annotating high confidence microRNAs using deep sequencing data. *Nucleic Acids Res* **42**, D68–73 (2014).
12. Lu, M. *et al.* miRNA-133 augments coelomocyte phagocytosis in bacteria-challenged *Apostichopus japonicus* via targeting the TLR component of IRAK-1 *in vitro* and *in vivo*. *Sci Rep* **5**, 12608 (2015).
13. Yang, L., Yang, G. & Zhang, X. J. The miR-100-mediated pathway regulates apoptosis against virus infection in shrimp. *Fish Shellfish Immunol* **40**, 146–153 (2014).
14. Bandyopadhyay, S. *et al.* MicroRNA-133a-1 regulates inflammasome activation through uncoupling protein-2. *Biochem Biophys Res Commun* **439**, 407–412 (2013).
15. Hou, J. *et al.* MicroRNA-146a feedback inhibits RIG-I-dependent Type I IFN production in macrophages by targeting TRAF6, IRAK1, and IRAK2. *J Immunol* **183**, 2150–2158 (2009).
16. Xiao, C. & Rajewsky, K. MicroRNA control in the immune system: basic principles. *Cell* **136**, 26–36 (2009).
17. Ma, X., Buscaglia, L. E. B., Barker, J. R. & Li, Y. MicroRNAs in NF- $\kappa$ B signaling. *J Mol Cell Biol* **3**, 159–166 (2011).
18. Dai, L., Gu, L. Y. & Di, W. MiR-199a attenuates endometrial stromal cell invasiveness through suppression of the IKK/NF- $\kappa$ B pathway and reduced interleukin-8 expression. *Mol Hum Reprod* **18**, 136–145 (2012).
19. Zhang, G. *et al.* The oyster genome reveals stress adaptation and complexity of shell formation. *Nature* **490**, 49–54 (2012).
20. Zhang, T. *et al.* The specifically enhanced cellular immune responses in Pacific oyster (*Crassostrea gigas*) against secondary challenge with *Vibrio splendidus*. *Dev Comp Immunol* **45**, 141–150 (2014).
21. Henneke, P. & Golenbock, D. T. Phagocytosis, innate immunity, and host-pathogen specificity. *J Exp Med* **199**, 1–4 (2004).
22. Kuchel, R. P., Aladaileh, S., Birch, D., Vella, N. & Raftos, D. A. Phagocytosis of the protozoan parasite, *Marteilia sydneyi*, by Sydney rock oyster (*Saccostrea glomerata*) hemocytes. *J Invertebr Pathol* **104**, 97–104 (2010).
23. Montagnani, C., Labreuche, Y. & Escoubas, J. M. Cg-I $\kappa$ B, a new member of the I $\kappa$ B protein family characterized in the pacific oyster *Crassostrea gigas*. *Dev Comp Immunol* **32**, 182–190 (2008).
24. Montagnani, C., Kappler, C., Reichhart, J. M. & Escoubas, J. M. Cg-Rel, the first Rel/NF- $\kappa$ B homolog characterized in a mollusk, the Pacific oyster *Crassostrea gigas*. *FEBS Letters* **561**, 75–82 (2004).
25. Zhang, Y., He, X. & Yu, Z. N. Two homologues of inhibitor of NF-kappa B (I $\kappa$ B) are involved in the immune defense of the Pacific oyster, *Crassostrea gigas*. *Fish Shellfish Immunol* **30**, 1354–1361 (2011).
26. Xu, F. *et al.* CgI $\kappa$ B3, the third novel inhibitor of NF-kappa B (I $\kappa$ B) protein, is involved in the immune defense of the Pacific oyster, *Crassostrea gigas*. *Fish Shellfish Immunol* **46**, 648–655 (2015).
27. Zhou, Z. *et al.* The identification and characteristics of immune-related microRNAs in haemocytes of oyster *Crassostrea gigas*. *PLoS One* **9**, e88397 (2014).
28. Canesi, L., Gallo, G., Gavioli, M. & Pruzzo, C. Bacteria-hemocyte interactions and phagocytosis in marine bivalves. *Microsc Res Techniq* **57**, 469–476 (2002).
29. Rodrick, G. E. & Ulrich, S. A. Microscopical studies on the hemocytes of bivalves and their phagocytic interaction with selected bacteria. *Helgoland Mar Res* **37**, 167–176 (1984).
30. Albert, S. & Baldwin, J. The NF- $\kappa$ B and I $\kappa$ B proteins: new discoveries and insights. *Annu Rev Immunol* **14**, 649–681 (1996).
31. Pauley, K. M. & Chan, E. K. MicroRNAs and their emerging roles in immunology. *Ann N Y Acad Sci* **1143**, 226–239 (2008).
32. Lewis, B. P., Burge, C. B. & Bartel, D. P. Conserved seed pairing, often flanked by adenosines, indicates that thousands of human genes are microRNA targets. *Cell* **120**, 15–20 (2005).
33. Bazzini, A. A., Lee, M. T. & Giraldez, A. J. Ribosome profiling shows that miR-430 reduces translation before causing mRNA decay in zebrafish. *Science* **336**, 233–237 (2012).
34. Shabalina, S. A. & Koonin, E. V. Origins and evolution of eukaryotic RNA interference. *Trends Ecol Evol* **23**, 578–587 (2008).
35. Axtell, M. J., Westholm, J. O. & Lai, E. C. Vive la différence: biogenesis and evolution of microRNAs in plants and animals. *Genome Biol* **12**, 221–233 (2011).
36. Iyori, M. *et al.* Resveratrol modulates phagocytosis of bacteria through an NF- $\kappa$ B-dependent gene program. *Antimicrob Agents Chem* **52**, 121–127 (2008).
37. Maiuri, M. C. *et al.* Nuclear Factor- $\kappa$ B regulates inflammatory cell apoptosis and phagocytosis in rat carrageenin-sponge implant model. *Am J Pathol* **165**, 115–126 (2004).
38. Ren, S. *et al.* NF- $\kappa$ B p65 and c-Rel subunits promote phagocytosis and cytokine secretion by splenic macrophages in cirrhotic patients with hypersplenism. *Int J Biochem Cell Biol* **45**, 335–343 (2013).
39. Tarver, J. E. *et al.* miRNAs: Small Genes with Big Potential in Metazoan Phylogenetics. *Mol Biol Evol* **30**, 2369–2382 (2013).
40. Marco, A., Hooks, K. & Griffiths-Jones, S. Evolution and function of the extended miR-2 microRNA family. *RNA Biol* **9**, 242–248 (2012).
41. Liu, R. *et al.* Identification and characterisation of pathogenic *Vibrio splendidus* from Yesso scallop (*Patinopecten yessoensis*) cultured in a low temperature environment. *J Invertebr Pathol* **114**, 144–150 (2013).
42. Shi, X. W. *et al.* The immunomodulation of acetylcholinesterase in zhikong scallop *Chlamys farreri*. *PLoS One* **7**, e30828 (2012).
43. Zhang, L. L., Li, L. & Zhang, G. F. A *Crassostrea gigas* Toll-like receptor and comparative analysis of TLR pathway in invertebrates. *Fish Shellfish Immunol* **30**, 653–660 (2011).
44. Livak, K. J. & Schmittgen, T. D. Analysis of relative gene expression data using real-time quantitative PCR and the 2<sup>- $\Delta\Delta$ CT</sup> method. *Methods* **25**, 402–408 (2001).
45. Wang, M. Q. *et al.* A primitive Toll-like receptor signaling pathway in mollusk Zhikong scallop *Chlamys farreri*. *Dev Comp Immunol* **35**, 511–519 (2011).

## Acknowledgements

We thank to Dr. Sudha Kappalli from Sree Narayana College, India, for discussions and critical reading of the manuscript, and the authors were also grateful to all the laboratory members for continuous technical advice and helpful discussion. This research was supported by the earmarked funds for Modern Agro-industry Technology Research System (CARS-48), the Taishan Scholar Program of Shandong.

### Author Contributions

H.C. carried out the molecular lab work and data analysis, participated in the design of the study and drafted the manuscript. W.L.W. carried out part of molecular lab work. Z.Z., H.W., R.L. and L.M.Q. participated in the design of the study and discussed the results. L.L.W. and L.S.S. conceived of the study, designed the study, coordinated the study and helped draft the manuscript. All authors gave final approval for publication.

### Additional Information

**Supplementary information** accompanies this paper at <http://www.nature.com/srep>

**Competing financial interests:** The authors declare no competing financial interests.

**How to cite this article:** Chen, H. *et al.* An invertebrate-specific and immune-responsive microRNA augments oyster haemocyte phagocytosis by targeting CgI $\kappa$ B2. *Sci. Rep.* **6**, 29591; doi: 10.1038/srep29591 (2016).



This work is licensed under a Creative Commons Attribution 4.0 International License. The images or other third party material in this article are included in the article's Creative Commons license, unless indicated otherwise in the credit line; if the material is not included under the Creative Commons license, users will need to obtain permission from the license holder to reproduce the material. To view a copy of this license, visit <http://creativecommons.org/licenses/by/4.0/>